Solar neutrino interactions with the double-β decay nuclei ^{82}Se, ^{100}Mo, and ^{150}Nd

H. Ejiri and S. R. Elliott

Solar neutrino interactions with the double beta decay nuclei of ^{82}Se, ^{100}Mo and ^{150}Nd

H. Ejiri[1] and S.R. Elliott[2]

[1]*Research Center for Nuclear Physics, Osaka University, Ibaraki, Osaka 567-0047, Japan*
[2]*Los Alamos National Laboratory, Los Alamos, NM, USA*

Solar neutrinos interact within double-beta decay ($\beta\beta$) detectors and contribute to backgrounds for $\beta\beta$ experiments. Background contributions due to solar neutrino interactions with $\beta\beta$ nuclei of ^{82}Se, ^{100}Mo, and ^{150}Nd are evaluated. They are shown to be significant for future high-sensitivity $\beta\beta$ experiments that may search for Majorana neutrino masses in the inverted-hierarchy mass region. The impact of solar neutrino backgrounds and their reduction are discussed for future $\beta\beta$ experiments.

Key words: solar-ν interaction, double beta decay, solar-ν backgrounds, neutrino mass sensitivity.

I. INTRODUCTION

Neutrino-less double beta decay ($\beta\beta(0\nu)$) is a unique and realistic probe for studies of neutrino (ν) properties and especially the Majorana mass character of the neutrino and the absolute mass scale. $\beta\beta$ studies and ν masses are discussed in recent reviews and their references [1–4].

The rate of $\beta\beta(0\nu)$, if it exists, would be extremely small because $\beta\beta$ is a second-order weak process that requires lepton number conservation violation and Majorana fermions. There are numerous possible mechanisms that can give rise to $\beta\beta(0\nu)$ as is discussed in the reviews[1–4]. It is known, however, that light neutrinos exist and therefore it is convenient to consider light-neutrino exchange as the default process by which to benchmark $\beta\beta(0\nu)$ rates. For light-neutrino exchange, the rate depends on the effective Majorana mass squared and the typical mass regions to be explored are about 45-15 meV and 4-1.5 meV in cases of the inverted-hierarchy (IH) and normal-hierarchy (NH) mass regions, respectively. The $\beta\beta(0\nu)$ half-lives expected for these regions are near or greater than 10^{27} years, depending significantly on the nuclear matrix element (NME), including the effective axial weak coupling g_A. As a result, the $\beta\beta(0\nu)$ signal rate ($S_{\beta\beta}$) is near or less than a few counts per ton of $\beta\beta$ isotope per year (t y). Accordingly the background rate necessarily has to be around or less than one count per t y.

Solar-νs are omnipresent and cannot be shielded, and thus their charged current (CC) and neutral current (NC) interactions are potential background sources for high sensitivity $\beta\beta$ experiments as discussed in [5, 6] and references therein. In fact, it has been shown that solar-ν CC interactions with $\beta\beta$ isotopes like ^{100}Mo [7], ^{116}Cd [8] and ^{150}Nd [9] can be used for real-time studies of the low-energy solar-νs.

The $\beta\beta$ isotopes most often used or considered for high-sensitivity experiments are ^{76}Ge, ^{82}Se, ^{100}Mo, ^{130}Te, ^{136}Xe and ^{150}Nd. Here, we classify them into two groups. Group A consisting of ^{82}Se, ^{100}Mo and ^{150}Nd have a large solar-ν CC rate, whereas Group B consisting of ^{76}Ge, ^{130}Te and ^{136}Xe have a rather small solar-ν CC rate. In the previous paper [5], background contributions from CC solar-ν interactions were discussed for the 3 $\beta\beta$ nuclei in Group B. Solar-ν interactions with atomic electrons in $\beta\beta$ isotopes and liquid scintillators used for $\beta\beta$ experiments were considered in Refs. [1, 6, 10, 11].

The present paper aims to evaluate the background contributions for the 3 nuclei in Group A and discuss the impact on high sensitivity $\beta\beta$ experiments using them. The mechanics of these calculations are identical to those in Ref. [5], and we do not repeat all the details here.

II. SOLAR NEUTRINO BACKGROUNDS

The process of $\beta\beta$ decay from $^{Z-1}$A to $^{Z+1}$A via the intermediate nucleus ^{Z}A is shown in Eqn. 1. Solar νs can produce background to this signal primarily through CC interactions with $\beta\beta$ nuclei. The CC interaction produces background in two ways. First the CC interaction itself can produce a signal (B_{CC}) given by the promptly emitted e$^-$ and, if the resulting nucleus is in an excited state, a number of γ rays may be emitted as the nucleus relaxes to its ground state. Second, the resulting nucleus ^{Z}A can then β^- decay to $^{Z+1}$A by emitting a single β^- ray and possibly also γ ray(s) if the residual state is an excited state (B_{SB}). The interaction and decay schemes are shown in Fig. 1. The 3 processes are expressed as,

$$\beta\beta: \quad {}^{Z-1}A \ \rightarrow \ {}^{Z+1}A + \beta^- + \beta^- + Q_{\beta\beta}$$
$$CC: \quad {}^{Z-1}A + \nu \ \rightarrow \ {}^{Z}A + e^- + \gamma(s) + Q_\nu$$
$$SB: \quad {}^{Z}A \ \rightarrow \ {}^{Z+1}A + \beta^- + \gamma(s) + Q_\beta, \quad (1)$$

where $\beta\beta$, CC, and SB denote the double beta decay, the solar-ν CC interaction, and the single beta decay processes, respectively. The Q values for each are given as $Q_{\beta\beta}$, Q_ν, and Q_β respectively, as shown in Fig. 1.

We consider $\beta\beta$ detectors where the sum energy of the β and γ rays is measured. The $\beta\beta(0\nu)$ signature is a peak within the region of interest (ROI) at the $\beta\beta$ Q value ($E = Q_{\beta\beta}$). In contrast, the sum of the electron

FIG. 1: Schematic diagrams of the $\beta\beta$ of ^{Z-1}A to ^{Z+1}A, the solar-ν CC interaction on ^{Z-1}A and the electron (γ) decay to ^{Z}A, and the single β/γ decays of ^{Z}A to ^{Z+1}A. $Q_{\beta\beta}$, Q_β , Q_ν, and Q_e are the Q values for $\beta\beta$, β, ν CC and electron capture (EC), respectively.

energy (E_e) and any successive γ ray energy (E_γ) is a continuum spectrum for both the CC and SB processes. The backgrounds of interest are estimated by their yields within the ROI and therefore are sensitive to the detector's energy resolution. The energy width of the ROI is given by the FWHM resolution (ΔE) at the energy of the Q value. This ratio, defined as δ, is the fractional energy resolution at $E = Q_{\beta\beta}$. Certainly the kinematics and event topologies for the backgrounds discussed here may permit experimental techniques for rejection that go beyond just a sum energy cut. We cannot anticipate all possible rejection techniques, but instead estimate rates so that future efforts may better assess these backgrounds for a given experimental configuration. In fact, methods to reduce the solar-ν backgrounds do depend on the detector configuration and the β^- and γ decay scheme of the nucleus. We briefly discuss these later for individual nuclei.

A.   The $\beta\beta(0\nu)$ Rate

We first evaluate the $\beta\beta(0\nu)$ signal rate $S_{\beta\beta}$ for the light ν-mass process and then compare to estimated CC and SB background rates. Although there are numerous other potential $\beta\beta(0\nu)$ mechanisms, providing this rate estimate enables a comparison to the background rates. The $\beta\beta(0\nu)$ signal rate for the light Majorana-ν exchange

is written as [2, 4]

$$S_{\beta\beta} = ln2\ G_{0\nu}(m_{eff})^2[M_{0\nu}]^2\epsilon_{\beta\beta}\frac{6\times10^{29}}{A}\ /\text{t y}, \quad (2)$$

where $S_{\beta\beta}$ is the signal rate per ton per year (t y) of the $\beta\beta$ isotope, $G_{0\nu}$ is the phase space volume, m_{eff} is the effective Majorana ν-mass in units of the electron mass, $\epsilon_{\beta\beta}$ is the $\beta\beta(0\nu)$ peak detection efficiency, and $M_{0\nu}$ is the nuclear matrix element (NME) for the light ν-mass process. Here $G_{0\nu}$ includes conventionally the axial weak coupling $g_A = 1.267g_V$ with g_V being the vector coupling constant, and $M_{0\nu}$ is given by the sum of the axial-vector and the vector NMEs.

The NMEs are expressed as $M_A = (g_A^{eff}/g_A)M_A^m$ and $M_V = (g_V^{eff}/g_V)M_V^m$, where M_A^m and M_V^m are model NMEs and (g^{eff}/g) are the renormalization (quenching) factors due to such non-nucleonic (isobar, exchange current etc) and nuclear medium effects that are not explicitly included in the model NMEs [2, 4, 12]. In a typical case of $G_{0\nu} = 5\times10^{-14}$/y, $m_{eff} = 20$ meV/m_e, $M_{0\nu}$=2, A=100, and $\epsilon_{\beta\beta}$=0.6, the $\beta\beta(0\nu)$ signal rate is $S_{\beta\beta} \approx 1$/t y.

B.   The β Decay of ^{Z}A

Next, we evaluate the background rate for the SB case. For SB, all solar-ν sources exciting the intermediate states below the neutron threshold energy B_n in ^{Z}A contribute to the production of the ground state of ^{Z}A via γ decay. Hence the production rate for ^{Z}A is given by the total solar-ν capture rate in units of SNU (S_t). The background rate per ton year for SB (B_{SB}) is expressed as

$$B_{SB} = 3.15\times10^{-29}n_{\beta\beta}S_t\epsilon_{SB}, \quad (3)$$

where $n_{\beta\beta}$ is the number of $\beta\beta$ isotope nuclei per ton, and ϵ_{SB} is the effective efficiency for the SB signal being located at the ROI after various cuts.

The solar-ν capture rates for individual neutrino sources are evaluated by using the neutrino responses $(B(GT), B(F))$ given by recent charge exchange reactions [13–15] and the neutrino fluxes from BP05(OP) [16]. The CC neutrino responses, $B(GT)$, have been studied by using high energy-resolution experiments at RCNP Osaka. The calculations were done as in Ref. [5] including the treatment of ν oscillations. The $\beta\beta$, solar-ν interaction, and single β Q values and the solar-ν capture rates for Group A nuclei are shown together with those for Group B nuclei [5] in Table I.

S_t for Group A and B nuclei are plotted against the neutrino CC Q_ν value in Fig. 2. The Group A nuclei of ^{82}Se, ^{100}Mo and ^{150}Nd with small negative Q_ν values around -170 keV, have large solar-ν capture rates because they are strongly excited by the pp neutrinos. On the other hand Group B nuclei of ^{76}Ge, ^{130}Te and ^{136}Xe have rather small solar-ν CC rates because the threshold

TABLE I: $\beta\beta$, CC, and SB Q values in units of MeV and solar-ν capture rates in units of SNU for selected $\beta\beta$ nuclei including the effect of oscillations. Column 8 gives S_t for no oscillations. $Q_{\beta\beta}$ is the $\beta\beta$ Q value, Q_ν is the ν-CC Q value for the lowest 1^+ state, Q_β is the single β Q value, S_B is the ^{8}B-ν capture rate, and S_t is the total solar-ν capture rate. The background rates for β decay (B_{SB}) and $\beta\beta(2\nu)$ ($B_{2\nu}$) are calculated for $\delta = 0.02$. The small differences in solar-ν capture rates in this table compared those reported in Ref. [5] are due to a small arithmetic error in the ^{7}Be flux calculations in that previous paper.

Isotope	$\beta\beta(2\nu)$ $\tau_{1/2}$ years	$Q_{\beta\beta}$ MeV	Q_ν MeV	Q_β MeV	S_{pp} (SNU)	S_B (SNU)	S_t no osc. (SNU)	S_t (SNU)	B_{SB} events/ t y	$B_{2\nu}$ events /t y
^{82}Se	9.2×10^{19} [17]	2.992	-0.172	3.093	257	10.0	672	368	4.42	0.15
^{100}Mo	7.1×10^{18} [17]	3.034	-0.168	3.202	391	6.0	975	539	0.11	1.56
^{150}Nd	8.2×10^{18} [17]	3.368	-0.197	3.454	352	15.5	961	524	0.12	1.00
^{76}Ge	1.93×10^{21} [18]	2.039	-1.010	2.962	0	5.0	15.7	6.3	0.03	0.005
^{130}Te	6.9×10^{20} [17]	2.528	-0.463	2.949	0	6.1	67.7	33.7	0.48	0.01
^{136}Xe	2.19×10^{21} [17]	2.468	-0.671	2.548	0	9.8	136	68.8	0.55	0.003

energy ($-Q_\nu$) is large enough that the pp neutrinos can not excite them. The pp neutrino contributions to the total capture rates for the Group A nuclei are around 60% of the total, while the ^{7}Be and ^{8}B neutrino capture rate are around 30% and 3%, respectively.

FIG. 2: Solar-ν capture rates in units of SNU for current $\beta\beta$ nuclei are plotted against the neutrino CC Q_ν value for the lowest 1^+ state. S_t is the total capture rate. Group A nuclei have a large S_t. Group B nuclei have a small S_t. .
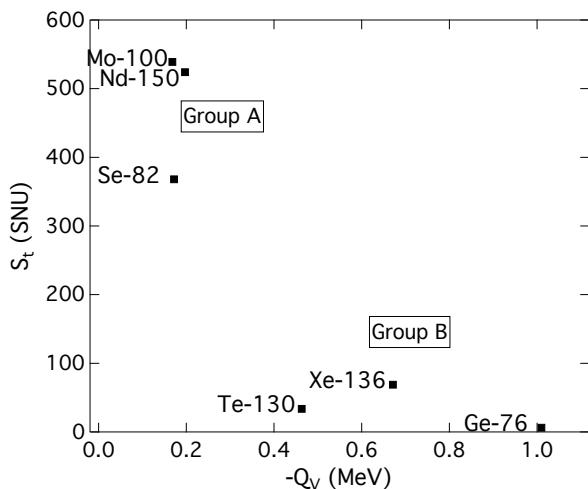
ϵ_{SB} is evaluated as a function of δ for simple calorimetric detectors. The background rates are approximately proportional to the resolution, i.e. the width of the ROI. B_{SB} for a fractional resolution of $\delta = 0.02$ are given in Table I.

For the cases of ^{100}Mo and ^{150}Nd, the ROI is located near the end-point energy at the tail of the single β-ray spectrum because $Q_{\beta\beta}$ is very close to Q_β. As a result, ϵ_{SB} is much reduced and B_{SB} is small for these nuclei. In the case of ^{82}Se, however, the intermediate nucleus ^{82}Br

decays primarily to the highly excited state at 2.648 MeV. Thus the ROI is located at the middle of the single β-ray energy spectrum resulting in ϵ_{SB} being relatively large, and a correspondingly large B_{SB}. B_{SB} for the Group A nuclei are also given in Table I.

1. ^{82}Se

The oscillated solar ν capture rate on ^{82}Se is calculated to be 368 SNU. ^{82}Br decays with a 98.5% branching ratio to the 2.648-MeV state in ^{82}Kr and this was the only state considered in our calculations. The ϵ_{SB} for decay of the ^{82}Br product to populate the ROI was calculated to be 2.6%, 5.2% and 15.7% for resolutions of $\delta = 0.01$, 0.02 and 0.05 respectively. The resulting SB spectrum is shown in Fig. 3.

FIG. 3: The sum spectrum of β and γ-ray energies for the decay of ^{82}Br. The hatched region shows the ROI fraction for a $\delta = 0.02$. .
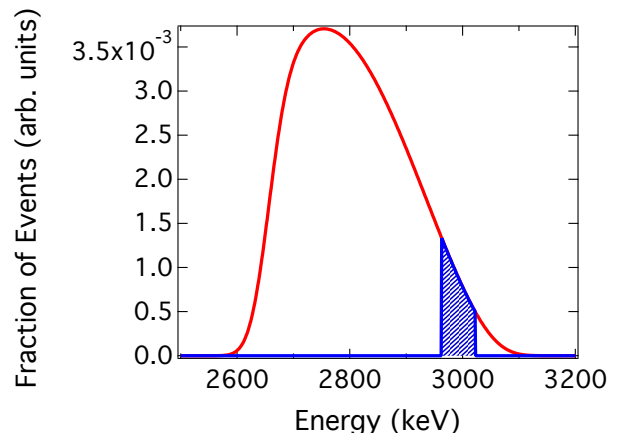
2. ^{100}Mo

The oscillated solar ν capture rate on ^{100}Mo is calculated to be 539 SNU. ^{100}Tc decays with a 93% branching ratio of to the ground state of ^{100}Ru and 5.7% to 1130-keV state. These were the only states considered in our calculations. The ϵ_{SB} for decay of the ^{100}Tc product to populate the ROI was calculated to be 0.06%, 0.1% and 0.3% for resolutions of $\delta = 0.01$, 0.02 and 0.05 respectively. The resulting SB spectrum is shown in Fig. 4.

FIG. 4: The sum spectrum of β and γ-ray energies for the decay of ^{100}Tc. The hatched region shows the ROI fraction for a $\delta = 0.02$. .
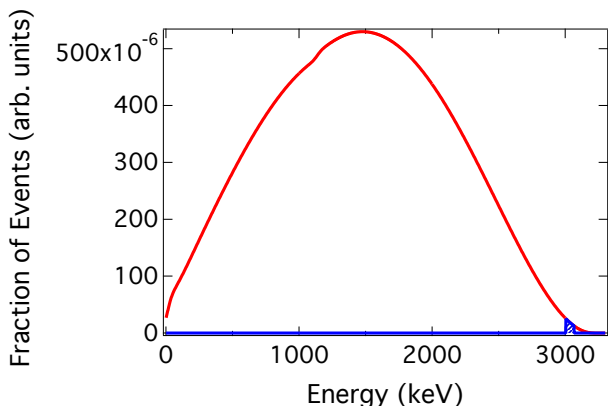
3. ^{150}Nd

The oscillated solar ν capture rate on ^{150}Nd is calculated to be 524 SNU. ^{150}Pm decays to numerous excited states in ^{150}Sm. We included all states to a branching ratio of 1% for a total branching ratio of 99.7%. However, the branching ratio to the ground state is uncertain and we took its value to be the upper limit value of 10%. There were 12 states included in our calculations. The ϵ_{SB} for decay of the ^{150}Pm product to populate the ROI was calculated to be 0.08%, 0.2% and 0.7% for resolutions of $\delta = 0.01$, 0.02 and 0.05 respectively. The resulting SB spectrum is shown in Fig. 5.

C. The Solar Neutrino CC Interaction

The ^{8}B ν spectrum extends to energies higher than $Q_{\beta\beta}$. Therefore energy deposits from ^{8}B solar-ν CC interactions at the ROI are possible. Hence, we consider CC reactions to the ith GT state in ^{Z}A at energy E_i above the ground state with e$^-$ emission followed by γ decays to the ground state in ^{Z}A. For simple calorimetric detectors, the sum energy of the CC produced e$^-$ energy (E_e)

FIG. 5: The sum spectrum of β and γ-ray energies for the decay of ^{150}Pm. The hatched region shows the ROI fraction for a $\delta = 0.02$. .
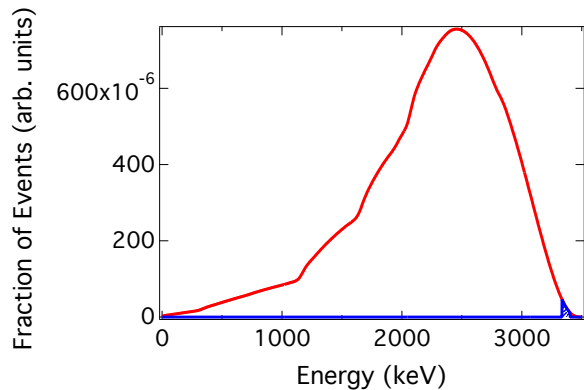
and any emitted γ-ray energy (E_γ) is measured. If the sum of these energies lies within the ROI at $Q_{\beta\beta}$, it will be a background to $\beta\beta(0\nu)$. The resulting values for E_ν and E_e are obtained from the condition, $E_e + E_i = Q_{\beta\beta}$, as;

$$E_\nu = Q_{\beta\beta} + Q_e, \quad E_e = Q_{\beta\beta} - E_i, \qquad (4)$$

where Q_e is the electron capture Q value for the ground state of ^{Z}A. Note for ^{82}Se, $Q_e = 171.7$ keV is the Q value for ν capture to the 75.1 keV meta-stable state in ^{82}Br, not the ground state as for the other nuclei under consideration here and correspondingly for this case, E_i is the energy from the meta stable state. The 5^- spin-parity assignment of the ^{82}Br ground state results in a negligible contribution to the CC interaction. The background rate due to ^{8}B-ν capture is obtained as

$$B_{CC} = \phi(^8B, E_\nu)\Delta E \sum_i \sigma(E_i), \qquad (5)$$

where $\phi(^8B, E_\nu)$ is the ^{8}B-ν flux per MeV at E_ν and $\sigma(E_i)$ is the neutrino CC cross section [5] to excite the ith GT state at E_i, and the sum extends over all GT states with $E_i \geq Q_{\beta\beta}$. B_{CC} is proportional to the fractional resolution $\delta = \Delta E/Q_{\beta\beta}$ because the fraction of the ^{8}B-ν flux contributing to the ROI is proportional to the width of the energy window.

These B_{CC} rates are smaller by 2-3 orders of magnitude than B_{SB} rates as given in Table I. Thus one may ignore the background contribution of B_{CC} for the present nuclei of the Group A as was done for the solar-ν backgrounds for the nuclei in the Group B [5].

III. SUMMARY AND DISCUSSION

The evaluated background rates for simple calorimetric detectors given in Table I are approximately 220 δ/t

y for ^{82}Se, 5.5 δ/t y for ^{100}Mo and 6.0 δ/t y for ^{150}Nd. In case of $\delta = 0.02$, they are, respectively, 4.42/t y, 0.11 /t y and 0.12/t y. For the case of δ=0.05, they are, respectively, 11/t y, 0.28/t y and 0.30/t y. Thus solar-ν backgrounds are serious for ^{82}Se experiments proposing to study the IH ν mass region unless the fractional resolution is reduced below 10^{-3}.

For experiments with modest resolution, $\beta\beta(2\nu)$ may also be a background at the ROI. Since this background ($B_{2\nu}$) and that of B_{SB} both depend on resolution, we compare the two. Using an approximation [21] for the number of $\beta\beta(2\nu)$ events that populate in the ROI, the number of background events for 2% fractional resolution is also given in Table I. Because the $\beta\beta(2\nu)$ half lives vary by a factor of ≈ 300 for these 6 isotopes, this background varies greatly also. For ^{100}Mo and ^{150}Nd, and to a lesser extent ^{82}Se, this is a significant issue for experiments approaching the ton scale and $B_{2\nu}$ dominates over B_{SB}. Therefore, the resolution of ^{100}Mo and ^{150}Nd detectors should be around 0.01 or less to avoid serious background from $\beta\beta(2\nu)$ to study the inverted hierarchy ν mass region. For ^{76}Ge, ^{130}Te, and ^{136}Xe $B_{2\nu}$ is small.

It is noted that fractional resolution of around 2% or less is required for the ^{130}Te and ^{136}Xe experiments to reduce B_{SB} in order to study the inverted hierarchy mass region.

So far, we have discussed selection of the true $\beta\beta(0\nu)$ signal and rejection of the background by only energy selection at the ROI in simple calorimetric detectors. Improvement of the energy resolution reduces the background rates by reducing the width ΔE of the ROI energy window. There are also several techniques to reduce ϵ_{SB} and hence B_{SB}. Each technique depends on specific detector configurations and thus we do not discuss such details in the present paper, but briefly describe possible reductions in general.

For solar-ν interactions on ^{82}Se and ^{150}Nd, the intermediate nuclei of ^{82}Br and ^{150}Pr decay primarily by emitting β and γ rays. One can reduce B_{SB} by measuring the spacial distribution of the energy deposits, since γ rays will interact in a much larger volume of the detector than the $\beta\beta(0\nu)$ signal. If detector segments are small, the γ rays detected outside the segment can be used to reject B_{SB} and B_{CC}.

Signal selection by time correlation (SSTC) can be used to reduce solar-ν background rates [2]. Since the half-life of the intermediate nucleus of ^{100}Tc is only 16 sec, B_{SB} in ^{100}Mo $\beta\beta$ experiments can be rejected by delayed anti-coincidence with the preceding CC e$^-$. This technique, however, is not useful for ^{82}Se and ^{150}Nd because of the long half-lives (35.3 hr and 2.68 hr, respectively) for the intermediate nuclei. In other wards, ^{100}Mo can be used to study pp solar-ν CC e$^-$ by a delayed coincidence with the successive SB β rays [7], but ^{82}Se and ^{150}Nd would be less effective as solar ν experiments.

Tracking detectors as used for real-time ^{82}Se and ^{100}Mo $\beta\beta$ experiments can be used to select $\beta\beta$ signals by measuring the individual two β rays [19, 20], and to reject B_{SB} with only one β ray. However, development of large tracking chambers with multi-ton scale enriched $\beta\beta$ isotopes is a real challenge for future.

Finally, it should be remarked that the ν-mass sensitivity for $\beta\beta$ experiments with NT t y of $\beta\beta$ isotope exposure is given by [2, 4, 21];

$$m_\nu < \frac{7.8 \text{ meV}}{M_{0\nu}}\sqrt{\frac{A}{G\epsilon}}\left(\frac{B}{NT}\right)^{1/4} \tag{6}$$

with constant G, A, $M_{0\nu}$, ϵ, B being the phase space in units of 10^{-14}/y, mass number, nuclear matrix element, detector efficiency, and background rate per year in the ROI per ton of $\beta\beta$ nuclei. Therefore one needs to optimize a number of key elements when planning future $\beta\beta$ experiments with the background being critical. The solar-ν background discussed here is just one of many components of the background, that needs to be considered for high-sensitivity $\beta\beta(0\nu)$ experiments hoping to cover the IH ν-mass region.

[1] S. Elliott S and J. Engel 2004 *J. Phys. G. Nucl. Part. Phys.* **30** R183
[2] H. Ejiri 2005 *J. Phys. Soc. Japan* **74** 2101
[3] F.T. Avignone III, S.R. Elliott S and J. Engel 2008 *Rev. Mod. Phys.* **80** 481
[4] J. Vergados, H. Ejiri, F. Šimkovic 2012 *Rep. Prog. Phys.* **75** 106301
[5] H. Ejiri and S. Elliott 2014 *Phys. Rev. C* **89** 055501
[6] N.F. de Barros and K. Zuber 2011 *J. Phys.* G **38** 105201
[7] H. Ejiri et al. 2000 *Phys. Rev. Lett.* **85** 2917.
[8] K. Zuber 2003 *Phys. Lett. B* **571** 148

[9] K. Zuber 2012 *Phys. Lett. B* **709** 6
[10] N.F. de Barros, J. Thurn, K. Zuber 2014 *J. Phys.* G **41** 115105
[11] H. Ejiri and K. Zuber 2016 *J. Phys. G* **43** 045201.
[12] H. Ejiri and J.I. Fujita 1978 *Phys. Rep.* **38**C 85.
[13] D. Frekers, et al. 2016 *Phys. Rev. C* **94** 014614.
[14] J.H. Thies et al., 2012 *Phys. Rev. C* **86** 044309.
[15] C.S. Guess et al., 2011 *Phys. Rev. C* **83** 064318.
[16] J.N. Bahcall, A.M. Serenelli, and S. Basu, Astrophys. J. Lett. 621, L85 (2005).
[17] A.S. Barabash, Nucl. Phys. A **935** 52, (2015).

[18] M. Agostino et al., Eur. Phys. J. C **75** (2015) 416.

[19] H. Ejiri et al. 2001 *Phys. Rev.* C **63** 065501.

[20] C. Arnaboldi et al. 2005 *Phys. Rev. Lett.* **95** 142501.

[21] S.R. Elliott and P. Vogel, Annu. Rev. Nucl. Part. Sci. **52**, 115 (2002).